

Far-infrared conductivity and anomalous below-gap absorption in superconducting granular NbN

D. R. Karecki, G. L. Carr, and S. Perkowitz
Physics Department, Emory University, Atlanta, Georgia 30322

D. U. Gubser and S. A. Wolf
Naval Research Laboratory, Washington, D.C. 20375
 (Received 26 January 1983)

The far-infrared ($10\text{--}100\text{ cm}^{-1}$) complex conductivity of superconducting granular NbN films has been determined from reflection and transmission data. Moderately granular films, with $R_{\square}=150$ and $200\ \Omega/\square$, followed Leplae-modified Bardeen-Cooper-Schrieffer-theory predictions with no absorption below the gap frequency ω_g . The derived values of $2\Delta/kT_c$ were 3.8 and 4.0, slightly below the results for homogeneous films. Highly granular films, with $R_{\square}\geq 500\ \Omega/\square$, displayed dc resistive tails and evidence of Josephson coupling. The real part of the far-infrared conductivity was BCS-type for frequencies above ω_g but showed an anomalous absorption below ω_g . This excess absorption may arise from two-dimensional fluctuations in the form of vortices or from normal conducting regions mixed in with the superconducting grains.

I. INTRODUCTION

Granular superconducting films exhibit a variety of physical phenomena due largely to the two-dimensional (2D) nature of the films and the nearly zero-dimensional (0D) nature of the grains. Many investigations¹ have been concerned with dc transport properties and reveal that the transitions to the superconducting state are not simple. The broad resistive transitions with their long tails are believed to reflect an initial 0D fluctuation region for the individual grains followed by long-range ordering via Josephson coupling. Although long-range order in the strict sense is not possible in two dimensions, the resistive transitions do show scaling behavior typical of critical phenomena.² A Kosterlitz-Thouless³ type of topological transition has been suggested as a possible mechanism.⁴ In this paper we present far-infrared (ac transport) measurements on one such system, granular NbN, and compare them with previous results for homogeneous NbN. Far-infrared photon energies $\hbar\omega$ are comparable to gap energies ($2\Delta=\hbar\omega_g$) and transition energies (kT_c), so it is plausible that excitations connected with a transition are observable. Anomalous far-infrared behavior has already been observed in elemental granular superconductors.⁵

The degree of granularity in NbN can be altered, from as-sputtered homogeneous samples with sheet resistances R_{\square} of $10\text{--}100\ \Omega/\square$, to highly granular samples with R_{\square} near $10^4\ \Omega/\square$. The homogeneous

films are comparable to films of the *A15* compounds such as V_3Si and are even more strongly coupled so that analysis of the superconducting properties is difficult. Homogeneous NbN was studied by Karecki, Peña, and Perkowitz⁶ (hereafter called KPP). Their far-infrared transmission measurements could not be fitted using the calculations of Mattis and Bardeen (MB).⁷ However, without resorting to a full strong coupling treatment (Nam⁸), they achieved satisfactory fits with the use of Leplae's⁹ approach with a finite Drude scattering time τ . Fitted values for 2Δ and τ agreed well with other determinations.

In this paper we examine the far-infrared behavior of granular NbN samples with $R_{\square}(300\text{ K})$

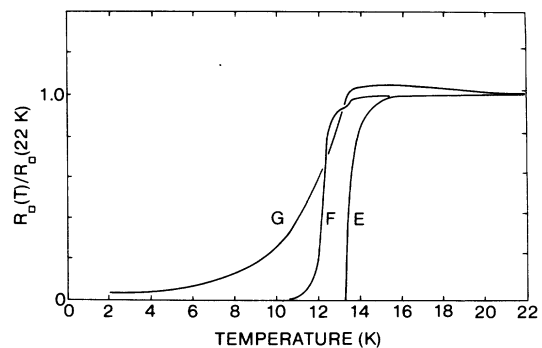


FIG. 1. Normalized dc sheet resistance vs temperature for granular NbN films showing the broadening of the superconducting transition with increasing granularity.

TABLE I. Experimentally measured and derived quantities for the homogeneous NbN samples *A*, *B*, and *C* considered by KPP and the anodized granular samples *D*, *E*, *F*, and *G* treated here. Thickness values are nominal. Uncertainties in R_{\square} and $Z(0)$ are no more than 10%, except that $Z(0)$ for sample *G* is known only to 20%. Values of 2Δ derived from the fits at 5.5 K have been extrapolated to the 0-K limit using the BCS result for the temperature dependence of 2Δ . This correction is less than 2%.

	<i>A</i>	<i>B</i>	<i>C</i>	Sample			<i>G</i>
				<i>D</i>	<i>E</i>	<i>F</i>	
d (nm)	100	30	20				2–3
$R_{\square}(300\text{ K})$ (Ω/\square)	8	52	65	150	200	500	8440
$R_{\square}(22\text{ K})$ (Ω/\square)	8	79	87	206	313	715	21 000
$Z(0)(22\text{ K})$ (Ω/\square)	8	79	87	180	240	400	2400
T_{c0} (K)	17	15	14	13.5	13.3	12.3	13.0
T_c (K)	17	15	14	13.5	13.3	10.5	<2
$2\Delta(0)$ (meV)	6.45	5.0	4.89	4.71	4.40		
$2\Delta(0)/k_B T_{c0}$	4.4	3.9	4.1	4.0	3.8		
τ (10^{-14} sec)	4.7	1.2	1.0	2.8	1.5		
$\omega_g \tau$	0.46	0.09	0.07	0.2	0.1		

=150–8440 Ω/\square . We find that samples with $R_{\square} < 500$ Ω/\square show Bardeen-Cooper-Schreiffer-type (BCS-type) behavior similar to that seen by KPP, but with 2Δ slightly reduced. Samples with $R_{\square} > 500$ Ω/\square , which have resistive tails, show unusual superconducting absorption for frequencies below the gap. Models for this new absorption are suggested although no quantitative fits are made. An important feature of our work is the measurement of both reflection and transmission, making it possible to obtain separate real and imaginary parts of the complex ac conductivity.

II. EXPERIMENT

Granular NbN samples were prepared at the Naval Research Laboratory. Four samples, typically 1×1 cm², were reactively sputtered onto sapphire substrates and then were anodized, a process which converts grain boundaries between NbN crystallites into insulating niobium oxides.¹⁰ The process conditions were chosen to produce samples with grains of ~ 8 nm diameter in a layer one grain deep. The oxide boundaries were estimated to be 1-nm wide. Two parallel strips of NbN were left unanodized to allow for resistance measurements. Table I displays basic properties of these samples (denoted *D*, *E*, *F*, and *G*) and of the homogeneous samples (denoted *A*, *B*, and *C*) studied by KPP.

In Fig. 1 we show resistance versus temperature $R(T)$ for samples *E*, *F*, and *G*. The curves exhibit three different behaviors. Sample *E* (and *D*, not shown) has a transition with no tail, like that observed by KPP in samples *A*–*C*, but at the lower temperature of 13.5 K. Sample *F* has a broader

transition with a large drop at 13.5 K and a small tail extending to 10.5 K. The minor structure just above 13.5 K is due to the small portion of unanodized NbN ($T_c = 14$ K) included within the voltage probes. Sample *G* has an extremely broad transition which has not yet reached completion at 2 K (possibly due to a lack of complete shielding). In Table I we indicate T_{c0} , the point of maximum slope in $R(T)$, and T_c , the temperature at which the resistance goes to zero. T_{c0} is associated with ordering on the individual grains and T_c with ordering of the entire sample. The superconducting I - V properties for the highly granular samples *F* and *G* are very similar to those described by Gubser *et al.*¹¹ From just above T_{c0} to 300 K, these two samples show an increasing conductivity consistent with thermally activated hopping. Sample *G* is also non-Ohmic at low temperatures ($T \cong 20$ K).

The far-infrared measurements were carried out with the use of a Grubb-Parsons Cube interferometer with a mercury-arc-lamp source and a helium-cooled bolometer-type detector operating at 1.8 K. Additional source-collimating optics and wire-grid polarizing beam splitters have improved the low-frequency sensitivity since the work of KPP. The spectral resolution was chosen to exclude interference effects arising from internal reflections in the sample substrate. The frequency range was 10–100 cm⁻¹ extending to 3 times ω_g . Sample cooling was accomplished with a Helitran system having a low-temperature limit of 5.5 K, well below T_{c0} for all the samples. Normal-state measurements were made at 22 K. The normal and superconducting transmission (T_n, T_s) and reflection coefficients were each measured.

III. THEORY

The success of KPP in fitting data for homogeneous NbN gives a starting point for the granular analysis. The ac conductivity in the superconducting state $\sigma_s(\omega) = \sigma_{1s} + i\sigma_{2s}$ can be derived from the normal-state conductivity $\sigma_n(\omega)$ if the ground state is BCS-type and the gap is frequency independent.^{8,9} A simple form for σ_n is the Drude result $\sigma_0/(1+i\omega\tau)$, where σ_0 is the dc conductivity. With this assumption for σ_n , the Leplae formulation gives σ_s/σ_n as a function of 2Δ and τ .

Tinkham¹² has shown that the far-infrared response of a thin film is completely determined by the ac surface impedance $Z(\omega) = 1/[\sigma(\omega)d]$, where d is the film thickness. In the Drude model the normal-state impedance is

$$Z(\omega) = \frac{(1+i\omega\tau)}{\sigma_0 d}. \quad (1)$$

Equation (1) has been confirmed for homogeneous films of V_3Si , Nb_3Ge , and Nb .¹³ The zero-frequency limit $Z(0)$ could be determined from dc sheet resistance measurements of $R_{\square} = 1/\sigma_0 d$ as well as from far-infrared transmission where $\omega\tau \ll 1$ since both methods gave the same result. $Z(0)$, together with appropriate values of τ and 2Δ , could then be used successfully to fit superconducting transmission data for V_3Si (Ref. 14) and for NbN samples *A*, *B*, and *C*.⁶

In using the same procedure for the granular films one complication that arises is that R_{\square} and $Z(0)$ no longer agree, as shown in Table I. Except for samples *A*, *B*, and *C* the two values increasingly diverge until for sample *G* they differ by a factor of 10. Such disagreement arises because a dc resistance measurement and a transmission measurement weigh the granularity in different ways. R_{\square} is strongly dependent on the lateral connectivity among the grains and would be infinite for grains separated by perfectly insulating regions. The same configuration would still produce a detectable effect in far-infrared transmission because each grain absorbs to give a finite value of $Z(0)$. [This argument suggests that $R_{\square} \geq Z(0)$ as observed in Table I.] For a dilute system the net transmission is just the area-weighted mean of the transmissions of the granular and insulating regions with the Drude form still applicable to the individual grains. The insulating region could contribute its own frequency behavior, but far-infrared measurements in a completely anodized film show no frequency dependence.

These considerations suggest that we continue to follow the Drude model and that we use $Z(0)$ rather than R_{\square} in fitting the data, since the former accounts for some of the optical averaging over grain

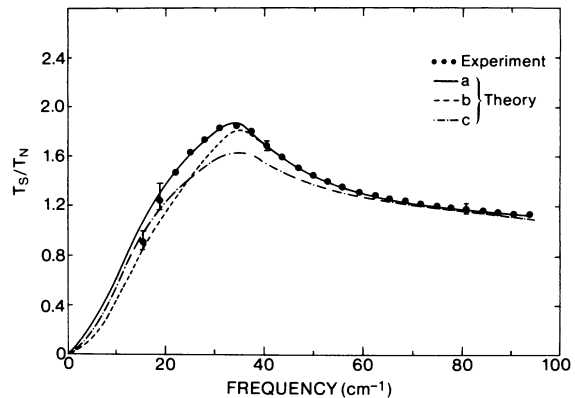


FIG. 2. T_s/T_n vs frequency for sample *E*. Curve *a* is calculated using the Leplae formulation of BCS theory and the Drude model with $2\Delta = 35.5 \text{ cm}^{-1}$, $\tau = 1.5 \times 10^{-14}$ sec, and the sheet resistance $Z(0) = 240 \text{ } \Omega/\square$ derived from T_n . Curve *b* is calculated from MB theory ($\tau = 0$) with the same 2Δ and $Z(0)$. Curve *c* is calculated from MB theory ($\tau = 0$) with the same 2Δ but $R_{\square} = 313 \text{ } \Omega/\square$.

and insulator properties (although only for $\omega\tau \ll 1$). With the Drude form for σ_n , the Leplae formulation to calculate σ_s/σ_n , and the value $Z(0)$, we can calculate all the necessary far-infrared properties. The main lack in our model is that it allows only the normal-state Drude frequency dependence and the corresponding superconducting-state frequency behavior. No new frequency dependences due to grain-grain or grain-insulator interactions can appear. As would be expected the model works well for samples with Drude-type normal-state properties but is less successful for other normal-state frequency dependences.

IV. RESULTS AND ANALYSIS

For samples *D* and *E*, T_n showed no more than a 10% decrease over the range 10–100 cm^{-1} . This decrease is probably due to the sapphire substrate, leaving a frequency-independent film transmission consistent with $\omega\tau \ll 1$ in the Drude model. The far-infrared behavior of sapphire at 22 K is not known with sufficient accuracy to allow a determination of τ . Our analysis deals with ratioed quantities such as T_s/T_n where the properties of the sapphire tend to cancel out.

The superconducting results for samples *D* and *E* are very similar and we discuss in detail only the latter. Figure 2 shows T_s/T_n for this sample and directly illustrates the importance of using $Z(0)$ instead of R_{\square} . The calculated peak height derived from R_{\square} and the MB conductivity is too low. An almost correct peak height is obtained by using the MB result and $Z(0)$. Finally, the introduction of

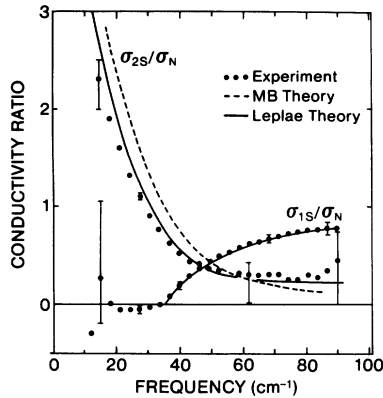


FIG. 3. Experimental and theoretical results for the conductivity ratios σ_{1s}/σ_n and σ_{2s}/σ_n for sample *E*. Experimental results have their greatest errors at the extremes of the frequency range. Solid and dashed curves are calculated, respectively, from the Leplae and MB theories with the values of 2Δ and τ used in Fig. 2. For σ_{1s}/σ_n the difference between the theories is negligible but becomes large for σ_{2s}/σ_n .

about the same τ value used previously for samples *B* and *C* by KPP, $\tau = 1.4 \times 10^{-14}$ sec ($\omega_g \tau = 0.1$), adjusts the curve width to give an excellent fit except at the lowest data point. The fit gives a gap value of 35.5 cm^{-1} .

The reflectivity of these samples is more sensitive to changes due to superconductivity than is that of samples with smaller values of R_{\square} . We could then derive experimental values for both σ_{1s} and σ_{2s} using the method of Palmer and Tinkham.¹⁵ (The method makes some approximations for multiple internal reflections which are not significant in our case.) The experimental results are shown in Fig. 3 along with several theoretical curves. The data for σ_{1s} show no absorption until the gap is reached at 35.5 cm^{-1} , the same value obtained from the fit to T_s/T_n . σ_{1s} is fitted equally well with either the MB or Leplae results which differ negligibly for $\omega_g \tau = 0.1$. MB theory is not successful in fitting σ_{2s} , however, while the Leplae result is much more satisfactory. The overall results for sample *D* are similar except that $\omega_g \tau = 0.2$.

Next we consider the highly granular samples *F* and *G*. T_n for these samples displayed non-Drude frequency dependences which were too large (a change of 25% between 20 and 100 cm^{-1}) to arise from the substrate and presumably represent granular behavior. T_s/T_n for both samples showed a BCS-type frequency dependence above the presumed gap frequency, but for $\omega < \omega_g$ behaved anomalously. The values were far lower than predicted from any acceptable combination of Leplae parameters, suggesting some additional absorption in the supercon-

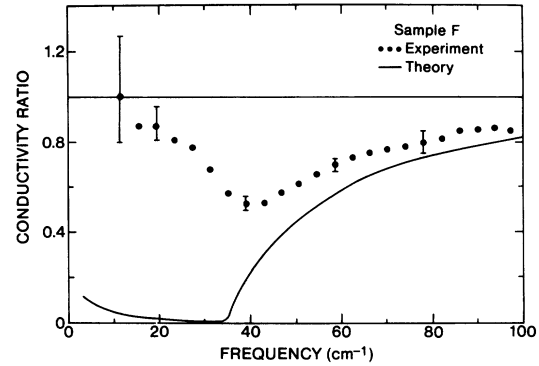


FIG. 4. Experimental and theoretical results for the conductivity ratio σ_{1s}/σ_n for sample *F*. Theoretical curve is calculated from MB theory with $2\Delta = 35.5$ cm^{-1} . Small rise in this curve at very low frequencies comes from the BCS quasiparticle term at finite T .

ducting state.

A more complete picture for this behavior comes from the combination of R and T data. The uncertainties in these quantities are such that the absorptive part of the conductivity, σ_{1s} , could be reliably determined, but σ_{2s} could not. In Figs. 4 and 5 we show σ_{1s}/σ_n for samples *F* and *G* along with the MB prediction. The frequency dependence of σ_{1s} is striking. For both samples the high-frequency trend follows the MB prediction but instead of approaching zero at and below the gap, σ_{1s} shows a large increase. For sample *G*, σ_{1s} for $\omega \leq 30$ cm^{-1} is actually greater than in the normal state. (To ensure that these anomalies are not an artifact of the conversion of R and T to σ_{1s} and σ_{2s} , we have also calculated the absorption coefficient $A = 1 - R - T$. This virtually directly measured quantity has no associated approximation or interpretation and shows similar below-gap behavior.) No BCS-based ap-

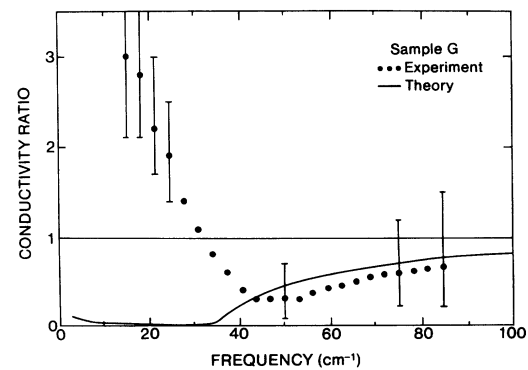


FIG. 5. Experimental and theoretical results for the conductivity ratio σ_{1s}/σ_n for sample *G*. Theoretical curve is calculated as in Fig. 4.

proach provides for absorption below ω_g (for $T \ll T_c$), which explains why T_s/T_n could not be fitted. The deviations from BCS behavior are so large that meaningful values of 2Δ and τ could not be found from a Leplae fit. For sample *F* we found that the additional absorption was smaller at 11 K than at 5.5 K.

V. DISCUSSION

Our results show three distinct categories for the NbN samples. The homogeneous films *A*, *B*, and *C* studied by KPP we classify as group I. These films are characterized by $R_{\square} < 100 \Omega/\square$, high values of T_{c0} and sharp resistive transitions. The normal-state infrared transmission is virtually frequency independent, while the superconducting state can be well described by the Leplae theory with $\omega_g\tau = 0.1-0.5$.

Samples *D* and *E* comprise the moderately granular group II. Their resistive transitions are somewhat rounded in a fashion consistent with 2D amplitude fluctuations.¹⁶ $R(T)$ then proceeds rapidly to zero with no evidence of a tail as T is reduced. The normal-state transmission is nearly frequency independent. Despite preliminary evidence for granularity [$R_{\square} \neq Z(0)$], the Leplae formalism gives reasonable fits to T_s/T_n when $Z(0)$ is used. The values obtained for 2Δ and $2\Delta/kT_c$, shown in Table I, are somewhat lower than for group I. The fit values for τ are similar to those obtained for samples *B* and *C*.

The last category, group III, includes films with $R_{\square} \geq 500 \Omega/\square$. The resistive transitions are even broader than for group II and show tails while the transition temperatures are further reduced. The normal-state transmission shows a non-Drude frequency dependence. The most striking feature is the appearance of absorption in the superconducting state for $\omega < \omega_g$. For $\omega > \omega_g$ the conductivity is BCS type, but no BCS-based theory (MB or Leplae) predicts a nonzero conductivity below the gap. This result is true independent of the form for $\sigma_n(\omega)$ chosen in the Leplae formulation. The additional absorption is stronger at 5 K than at 11 K.

The T_s/T_n ratios for group III have a shape similar to those observed by Carr *et al.*¹⁷ in granular Pb films. In that work, as the granularity of the film increased, the transmission ratio for frequencies at and below the gap decreased. For highly granular samples, the ratio was less than one, suggesting strong absorption for frequencies around the gap. Our observed additional absorption lies below the bulk gap but perhaps reflects the same mechanism.

At present, we have no definitive theory for below gap absorption. Few of the ideas developed to ac-

count for the dc properties have been extended to the far infrared in a quantitative way. The discussion below is provided to suggest directions for more detailed theoretical investigations.

Fluctuations in the amplitude of the superconducting order parameter can give rise to additional conductivity and therefore absorption. Two fluctuation regions can be defined, a 0D region around the grain transition temperature T_{c0} , and a 2D region around the final transition temperature T_c . In previous work¹⁸ 0D fluctuations were invoked to explain the temperature dependence of the far-infrared transmission of sample *G*. For $\omega < \omega_g$, a fluctuation conductivity calculated from Ginzberg-Landau theory gave the observed temperature dependence near T_{c0} where the BCS prediction was not followed. Here, our extended frequency data gives a large anomalous absorption nearly 2 orders of magnitude greater than the calculated value.¹⁹ Also, in sample *F*, the absorption increases for temperatures decreasing below T_c , inconsistent with fluctuation behavior.

Another possible mechanism for absorption below the gap involves interactions with superfluid vortices. In a 2D geometry, these vortices represent excitations which can be induced thermally or by the application of a small magnetic field (typically ≤ 1 mG). Absorption from the induced motion of the vortices results from the normal core region.²⁰ However, for temperatures below T_c , the vortices are expected to be pinned so that induced motion is unlikely. Absorption may still arise, however, if the photon energies are great enough to create vortex pairs, break apart bound pairs, or free vortices pinned to imperfections. In the absence of a complete frequency-dependent theory for vortices we note that a similar type of process has been suggested by Shirafuji *et al.*²¹ as an infrared detection mechanism in Nb microbridges. Their $I-V$ properties versus temperature show remarkable similarities to the NbN results of Gubser *et al.*¹¹ The Nb bridges were current-biased to just above the critical current so that a voltage, presumably due to flux flow, appeared. Incident infrared radiation then caused a voltage increase, which was attributed to a radiation-induced increase in vortex creation. The measured frequency response was found to be a broad peak centered around a frequency below ω_g , a shape which is not inconsistent with our measured absorption.

These vortex ideas suggest that the granular samples should display far-infrared detection. In preliminary measurements on sample *G* using an optically pumped far-infrared laser we measured a detection voltage at 18 cm^{-1} for temperatures at and below 4.5 K. However, it is not clear that this

detection is directly related to the observed low-frequency absorption.

Another possible explanation of the below-gap absorption has been offered by Garner and Stroud,²² who have used the effective-medium approximation²³ (EMA) to explore the behavior of a random 2D mixture of superconductor and normal metal. Our granular NbN samples may well approximate such a mixture since the particular niobium oxide which is expected to be in direct contact with the NbN grains, NbO, is known to be a reasonably good conductor.²⁴ The EMA calculation shows a percolation transition when the concentration of the more conductive component reaches 50%. Garner and Stroud have calculated the ac conductivity near percolation and find an absorptive part which is in qualitative agreement with our results for samples *F* and *G*. The theory also shows that σ_{1s}/σ_n can exceed unity near percolation, as observed in sample *G*. The resistive transition for this sample suggests that it is very close to the superconducting percolation concentration. At present we cannot make quantitative comparisons with EMA theory due to the lack of detailed knowledge of the optical properties of NbO. Further, the presence of a third component, the insulating oxide Nb₂O₅, is not yet incorporated in the model.

VI. CONCLUSIONS

We have measured far-infrared reflection and transmission for moderately and highly granular films of NbN. The moderately granular films ($R_{\square} = 150\text{--}200 \Omega/\square$) are Drude type in the normal state. Their superconducting behavior can be fitted if $Z(0)$ is used rather than R_{\square} and the experimental

result for σ_{1s}/σ_n follows BCS-based theory. The fitted values of τ are similar to those obtained for the homogeneous samples. The fitted values of $2\Delta/kT_c$ are slightly reduced from the homogeneous values. This result is not unexpected since the tunneling data of Saito *et al.*²⁵ show that $2\Delta/kT_c$ decreases with decreasing T_c . However, our values are somewhat below those reported by Saito *et al.* at the same transition temperatures, suggesting that granularity has some effect on the degree of strong coupling.

The highly granular films ($R_{\square} = 500\text{--}8440 \Omega/\square$) are not Drude type in the normal state. Their superconducting behavior is characterized by a large, distinctly non-BCS absorption below the gap. This absorption does not have the correct temperature or frequency dependence to arise from amplitude fluctuations of the order parameter. Two other possibilities, both intimately connected with the granularity of the system, are vortex absorption and superconductor-metal percolation behavior. The presence of vortices could lead to far-infrared detection and this is indeed observed in preliminary measurements in sample *G*. The percolation picture, derived by Garner and Stroud from a very simplified model using EMA theory, gives qualitative agreement with the observations. Further measurements and quantitative comparisons are needed to distinguish between these possibilities.

ACKNOWLEDGMENTS

The authors thank F. Family for helpful discussions. This work was supported by the U. S. Department of Energy under Contract No. DE-AS05-79ER10436.

¹A large number of articles pertaining to these systems may be found in *Inhomogeneous Superconductors—1979 (Berkeley Springs, W.V.)*, Proceedings of the Conference on Inhomogeneous Superconductors, edited by D. U. Gubser, T. L. Francavilla, J. R. Leibowitz, and S. A. Wolf (AIP, New York, 1980).
²S. A. Wolf, D. U. Gubser, and Y. Imry, Phys. Rev. Lett. **42**, 324 (1979).
³J. M. Kosterlitz and D. J. Thouless, J. Phys. C **6**, 1181 (1973).
⁴M. R. Beasley, J. E. Mooij, and T. P. Orlando, Phys. Rev. Lett. **42**, 1165 (1979).
⁵G. L. Carr, J. C. Garland, and D. B. Tanner, in *Inhomogeneous Superconductors—1979 (Berkeley Springs, W.V.)*, Ref. 1, p. 288.
⁶D. R. Kavecki, R. E. Peña, and S. Perkowitz, Phys. Rev. B **25**, 1565 (1982).
⁷D. C. Mattis and J. Bardeen, Phys. Rev. **111**, 412, (1958).

⁸S. B. Nam, Phys. Rev. **156**, 480 (1967); **156**, 487 (1967).
⁹L. Leplae, doctoral dissertation, University of Maryland, 1962 (unpublished).
¹⁰S. A. Wolf, J. Kennedy, and M. Nisenoth, J. Vac. Sci. Technol. **13**, 1451 (1976).
¹¹D. U. Gubser, S. A. Wolf, T. L. Francavilla, and J. L. Feldman, in *Inhomogeneous Superconductors—1979 (Berkeley Springs, W.V.)*, Ref. 1, p. 159.
¹²M. Tinkham, in *Far Infrared Properties of Solids*, edited by S. S. Mitra and S. Nudelman (Plenum, New York, 1970), p. 223.
¹³S. W. McKnight, R. H. Thorland, and S. Perkowitz, Thin Solid Films **41**, L61 (1977).
¹⁴S. W. McKnight, B. L. Bean, and S. Perkowitz, Phys. Rev. B **19**, 1437 (1979).
¹⁵L. H. Palmer and M. Tinkham, Phys. Rev. **165**, 588 (1968).
¹⁶L. G. Aslamasov and A. I. Larkin, Phys. Lett. **26A**, 238 (1968).

- ¹⁷G. L. Carr, doctoral dissertation, Ohio State University, 1982 (unpublished); G. L. Carr, J. C. Garland, and D. B. Tanner, *Bull. Am. Phys. Soc.* 26, 448 (1981).
- ¹⁸S. Perkowitz, *Phys. Rev. B* 25, 3420 (1982).
- ¹⁹D. B. Tanner, *Phys. Rev. B* 8, 5045 (1973).
- ²⁰J. Bardeen and M. J. Stephen, *Phys. Rev.* 140, A1197 (1965).
- ²¹J. Shirafuji, S. Matsui, H. Hida, K. Sakai, and Y. Inuishi, *Jpn. J. Appl. Phys.* 19, 2115 (1980).
- ²²J. Garner and D. Stroud (private communication).
- ²³D. A. G. Bruggeman, *Ann. Phys. (Leipzig)* 24, 636 (1935).
- ²⁴K. E. Gray, *Appl. Phys. Lett.* 27, 462 (1975).
- ²⁵Y. Saito, T. Anayama, Y. Onodera, T. Yamashita, K. Komenou and Y. Muto, in *Proceedings of the 12th International Conference on Low Temperature Physics, 1970*, edited by R. Kanda (Academic, Tokyo, 1971), p. 329.